iScience

Article

Unveiling pressure-induced anomalous shear behavior and thermoelasticity of α-Fe_2O_3 hematite at high pressure

Graphical abstract

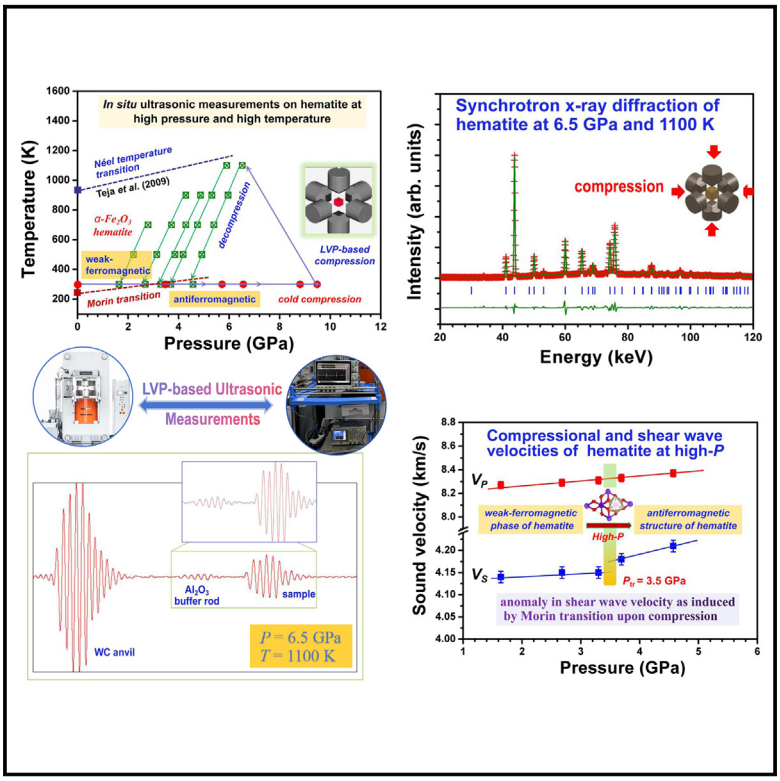

Highlights

- Revealing Morin transition-induced anomaly in the shear velocities of compressed hematite
- Yielding sound velocities and thermoelasticity of α-Fe_2O_3 hematite at high *P-T*
- Exploring the underlying mechanism for pressure-induced shear anomaly in Fe-O materials

Authors

Yongtao Zou, Pei Wang, Ying Li, Haiyan Chen, Cangtao Zhou, Tetsuo Irifune

Correspondence

zouyongtao@sztu.edu.cn

In brief

Materials science; Materials characterization; Magnetic materials; Materials physics

Zou et al., 2025, iScience *28*, 111905
February 21, 2025
https://doi.org/10.1016/j.isci.2025.111905

CellPress

iScience

CellPress
OPEN ACCESS

Article

Unveiling pressure-induced anomalous shear behavior and thermoelasticity of α-Fe_2O_3 hematite at high pressure

Yongtao Zou,[1,6,7,*] Pei Wang,[2,6] Ying Li,[3] Haiyan Chen,[4] Cangtao Zhou,[1] and Tetsuo Irifune[5]

[1]College of Engineering Physics, and Shenzhen Key Laboratory of Ultraintense Laser & Advanced Material Technology, Shenzhen Technology University, Shenzhen 518118, China

[2]Key Laboratory of Materials Physics, Institute of Solid State Physics, HFIPS, Chinese Academy of Sciences, Hefei 230031, China

[3]United Laboratory of High-Pressure Physics and Earthquake Science, Institute of Earthquake Forecasting, China Earthquake Administration, Beijing 100036, China

[4]Mineral Physics Institute, State University of New York, Stony Brook, NY 11790, USA

[5]Geodynamics Research Center, Ehime University, Matsuyama 790-8577, Japan

[6]These authors contributed equally

[7]Lead contact

*Correspondence: zouyongtao@sztu.edu.cn

https://doi.org/10.1016/j.isci.2025.111905

SUMMARY

Hematite (α-Fe_2O_3), as an important end-member of FeO-Fe_2O_3 series, has garnered particular interest for its peculiar high pressure-temperature (*P-T*) behavior, structural stability and elasticity, and the unclear role of Fe^{3+} in the nature and dynamics of the Earth's mantle. Here, we report a pronounced pressure-induced anomaly in the shear behavior of hematite at room temperature and ~3.5 GPa owing to the (weak)ferromagnetic-to-antiferromagnetic Morin transition driven by pressure and temperature. Unexpectedly, this phase-transition-driven anomalous behavior at high *P-T* is absent in the compressional velocities. The bulk and shear moduli, as well as their pressure and temperature dependences for Fe_2O_3 hematite are reported, yielding K_{S0} = 235.5(8) GPa, G_0 = 88.0(3) GPa, $\partial K_S/\partial P$ = 3.29(25), dG/dP = 1.36(10), $\partial K_S/\partial T$ = −0.027(2) GPa/K, and $\partial G/\partial T$ = −0.019(1) GPa/K. These findings and high-*P* thermoelasticity will be of significant importance for good understanding of the underlying mechanism for phase-transition-induced anomaly at high pressures and temperatures in the shear behavior of Fe-O materials.

INTRODUCTION

Iron-bearing oxides have attracted considerable interest and play an important role in materials science and mineralogy of the Earth's interior owing to their complex crystal structure, sound velocities, and magnetic and elastic properties under high pressure-temperature (*P-T*) conditions. Hematite (α-Fe_2O_3) mineral, as an important end-member of FeO-Fe_2O_3 series (i.e., FeO wüstite, Fe_2O_3 hematite, Fe_3O_4 magnetite, a new Fe_4O_5 compound), is of particular interest for the high *P-T* behaviors and properties of ferric oxides in the compositions, the unclear role of Fe^{3+} in the nature and dynamics of the Earth's mantle, as well as the technological applications.[1–14]

Under ambient conditions, hematite is a thermodynamically stable iron oxide with a corundum hexagonal-close-packed (*hcp*) crystal structure, where the Fe^{3+} cations are located in the distorted oxygen octahedra.[15] Below the Morin temperature (T_M) of ~263 K, Fe_2O_3 was preferred to adopt an antiferromagnetic (AFM) structure, and it transformed into a weakly ferromagnetic (FM) phase above its Morin temperature, owing to a slight canting in the alignment of the antiferromagnetic planes in corundum structure until the Néel temperature of ~948 K.[16–18] It was ever proposed that the pressure-temperature boundary of the Morin transition was quite sensitive to both the pressure environment and sample microstructure.[19–23] At high pressure, the T_M exhibited a dramatic rise and reached ~300 K upon compression up to 2–5 GPa, as determined by the variations in magnetic and elastic properties with pressures.[19–24]

To date, numerous studies on the structural evolution in compressed Fe_2O_3 have been carried out using various high-pressure techniques (e.g., dynamic shock-wave and static compression experiments); however, the crystal structure, phase stability and magnetic properties of Fe_2O_3 at high pressure still remain open questions.[3,6–10,12,23–26] For example, at pressures above ~50 GPa, α-Fe_2O_3 undergoes a first-order phase transition from the corundum-type hematite structure to a metallic high-pressure phase (also called Mott insulator-metal transition), which is accompanied by a remarkable volume collapse of ~10%.[3,6–10,12,23–26] Previous high-pressure X-ray diffraction and Mössbauer spectroscopy studies discovered a high-pressure new phase, which possessed an orthorhombic perovskite structure[9,23] (space group: *Pbnm*) and was controversial to the

recent result by Pasternak et al.[7] using the combined experimental techniques of X-ray diffraction, Mössbauer spectroscopy and electrical resistance measurements. As identified only from the X-ray diffraction observations, it is difficult to determine what the exact structure of the new high-pressure phase is? However, the recent Mössbauer spectroscopy measurements showed that only one Fe^{3+} site was observed in the new high-pressure phase, indicating that the new phase may be ascribed to the Rh_2O_3(II)-type structure, but not the orthorhombic perovskite-type one.[7]

Bulk and shear moduli and their pressure and temperature dependences of materials are important parameters in understanding their high *P-T* behaviors and physical properties.[27–31] The equation of state and compressibility/bulk modulus (K_0) of hematite have been studied by synchrotron-based static compression experiments and theoretical calculations;[9,19–21,29–31] however, these reported values were still quite scattered and not well constrained, ranging from 199 GPa to 241.7 GPa with the associated pressure derivative ($\partial K/\partial P$) ranging from 3.1 to 4.53.[9,19–21,29–31] Sound velocities and elasticity of single-crystal and polycrystalline hematite first have been measured at pressures up to 3 kbar and temperatures of 200∼300 K by Liebermann et al.[19,20] using the offline LVP-based ultrasonic measurements, where the changes in the elastic moduli (*i.e.*, bulk and shear moduli) across the magnetic Morin transition of T_M = 261 K for hematite at ambient pressure were discovered,[19] and the new elasticity data were reported as K_0 = 206.6 GPa and G_0 = 91.0 GPa with the associated pressure derivatives of K' = 4.53 and G' = 0.73.[20]

Despite the importance of iron-bearing oxides (i.e., FeO-Fe_2O_3 system), to date, most previous studies were focused on the phase transitions and/or compressibility/bulk modulus at high pressure and/or ambient temperature, only elucidating the nature of pressure-induced phase transformations and/or bulk modulus/density changes vs. pressures.[3,6–9,12,13] Very few attention have been devoted to studying the sound velocities and elasticity of α-Fe_2O_3 hematite at high pressure,[19,20] let alone at the simultaneous high-pressure and high-temperature conditions, especially in terms of the shear-related properties. In this study, simultaneous high-pressure and high-temperature sound-velocity measurements on polycrystalline α-Fe_2O_3 hematite are performed in a large volume press using the state-of-the-art technique of ultrasonic interferometry in conjunction with synchrotron X-ray diffraction and radiographic imaging.[32–37] Here, we reveal pressure-induced anomalies in the shear properties of Fe_2O_3 hematite and explore the underlying mechanism of the abnormal shear behavior at high pressure. An internally consistent set of new thermoelasticity data for hematite is also reported based on our currently measured sound velocities and densities data.

RESULTS

Synchrotron X-Ray diffraction, sound velocities, and phase-transition-induced anomaly in the shear behavior of α-Fe_2O_3 hematite at high pressure

The as-measured polycrystalline α-Fe_2O_3 hematite specimen used in the current study is provided by Robert C. Liebermann (Stony Brook University, USA). Acoustic sound wave velocities of polycrystalline α-Fe_2O_3 hematite were measured at simultaneously high pressures and temperatures using the state-of-the-art technique of ultrasonic interferometry combined with synchrotron X-ray radiation in a large volume press. The experimental setup and the pressure-temperature (*P-T*) path for the present synchrotron-based experiments are shown in Figures 1A and 1B, where each point represents a pressure-temperature (*P-T*) condition that X-ray diffraction and acoustic data for α-Fe_2O_3 hematite are collected. Details of the high *P-T* cell assembly can be found elsewhere.[32–37]

At ambient conditions, the polycrystalline Fe_2O_3 hematite possesses a hexagonal-close-packed (*hcp*) crystal structure, where the Fe^{3+} cations are located in distorted oxygen octahedra, as shown in Figure 1C. In this experiment, we performed five heating/cooling cycles at pressures and temperatures up to 6.5 GPa and 1,100 K, as shown in Figure 1B. The Fe_2O_3 hematite sample was annealed at the peak *P-T* conditions of each cycle for several minutes to release nonhydrostatic stress which was accumulated in the pressure chamber during cold compression. After annealing, we collected the data of ultrasonic travel times, X-ray diffraction pattern and x-radiographic imaging at each *P-T* conditions. Representative echo trains for the compressional wave (50 MHz) from the interfaces (e.g., between the anvil and buffer rod, the buffer rod and sample, and the sample and pressure marker) at the peak *P-T* conditions of 6.5 GPa and 1,100 K are shown in Figure 1D. It is found that the echoes from the aforementioned interfaces can be clearly identified, ensuring a precise determination of the compressional and shear travel times even at the highest *P-T* conditions.

Prior to the current synchrotron-based ultrasonic sound velocity measurement experiments, the polycrystalline hematite specimen is characterized by X-ray diffraction and SEM observations, showing that the as-measured hematite possesses a pure hexagonal-close-packed (*hcp*) structure [in Figure 2A] and is free of visible microcracks. The bulk density of Fe_2O_3 hematite specimen used in this study is ∼5.24(2) g/cm^3 as determined by the Archimedes immersion method, reaching ∼99.5% of the theoretical X-ray density of 5.267 g/cm^3. This means that the porosity of the specimen is about 0.5%, indicating a negligible effect of porosity on the elasticity of polycrystalline hematite within uncertainties.[30,33–35] After annealing and resintering the bulk hematite at the peak *P-T* conditions of 6.5 GPa and 1100 K, a typical X-ray diffraction pattern of hematite at 6.5 GPa and 1,100 K is collected (in Figure 2B), indicating that the specimen is still a corundum-structured material, and no other phases such as wüstite (FeO) or magnetite (Fe_3O_4) are observed throughout the current high *P-T* experiments.[38] Further SEM analyses of the hematite recovered from the current ultrasonic measurements show that the specimen exhibits an equilibrated and homogeneous microstructure with an average grain size of ∼500 nm (in Figure 2C). Energy-dispersive X-ray composition measurements (SEM-EDX) show that the recovered specimen possesses almost a stoichiometric Fe_2O_3 composition within uncertainties.

As shown in Figure 2D, the compressional (V_P) and shear (V_S) wave velocities of hematite at 300 K after annealing are plotted as a function of pressure. Clearly, the shear wave velocities (V_S) exhibit a pronounced pressure-induced discontinuity at

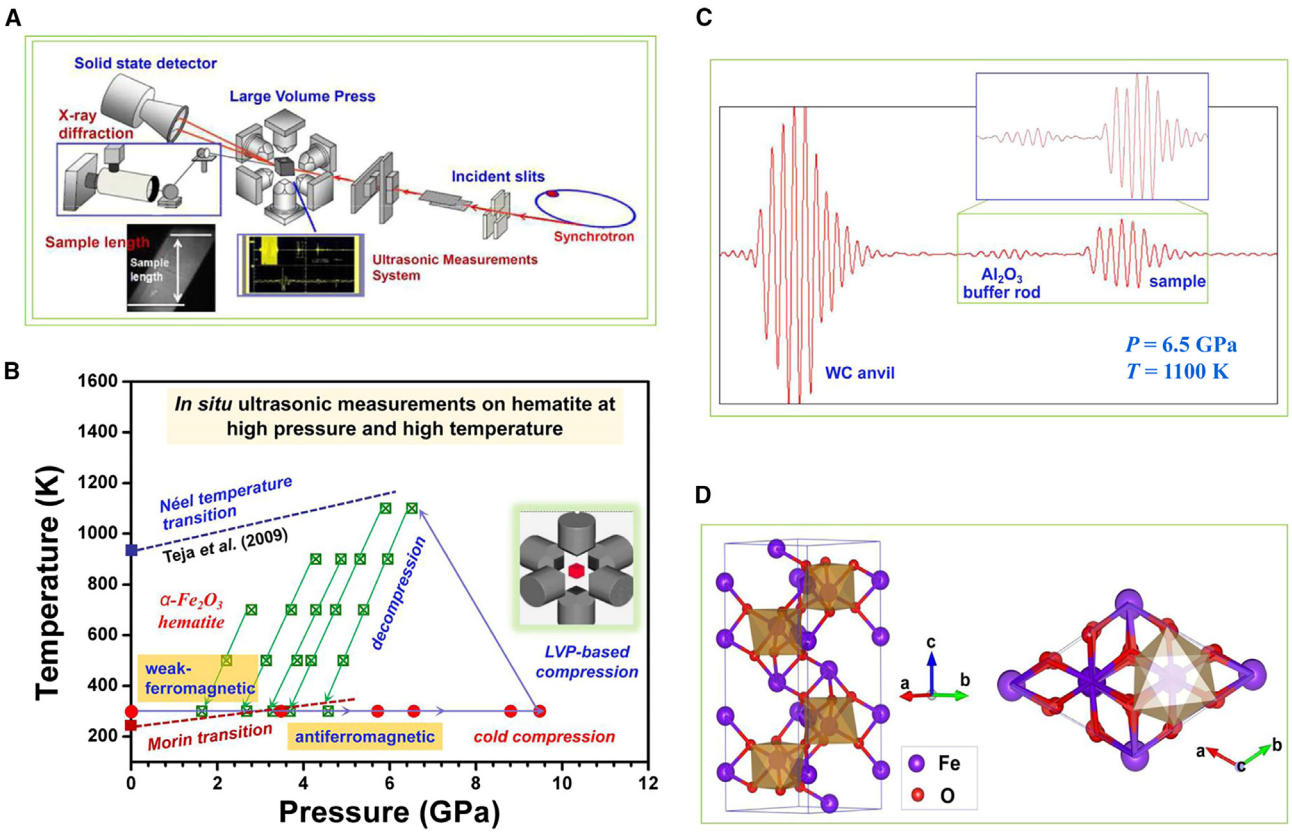

Figure 1. Synchrotron-based experimental setup, experimental *P-T* path, crystal structure, and representative ultrasonic echoes at high pressure and high temperatures of α-Fe_2O_3 hematite

(A) Experimental setup for the current ultrasonic interferometry measurements in conjunction with synchrotron X-ray diffraction in a multi-anvil high-pressure apparatus; (B) Experimental *P-T* conditions for the combination of ultrasonic interferometry and synchrotron X-ray diffraction measurements on polycrystalline α-Fe_2O_3 hematite, as well as the typical phase boundary for hematite at high pressure and low/high temperature based on the previous studies. The red circle symbols represent the current *P-T* data points upon cold compression, whereas the crossed-green-square symbols are those at high *P-T* conditions during cooling of this study. The navy blue dash line and square are the phase boundary for paramagnetic-to-ferromagnetic transition (Néel temperature) determined by Teja et al.[38] The Morin transition or Mott insulator-metal transition boundary is also shown here in a red dash line based on the recent study by Bezaeva et al.; (C) Crystal structure of α-Fe_2O_3 hematite at ambient conditions with a corundum hexagonal-close-packed (*hcp*) crystal structure, where the Fe^{3+} cations are located in distorted oxygen octahedra. Large Fe^{3+} ions at octahedral sites are represented by green spheres; and oxygen ions are symbolized by red spheres; (D) Representative waveform data for the compressional wave signal (50 MHz) at 6.5 GPa and 1,100 K, showing the reflections from the WC-anvil, the buffer rod, and the hematite sample.

$\sim$3.5 GPa and 300 K after annealing, which is absence in the compressional wave velocities (V_P) versus pressures up to $\sim$4.6 GPa. This pressure-induced anomalous behavior in shear wave velocity (V_S) is not due to the volume-related structural phase transition as identified by our synchrotron X-ray diffraction observations at high pressure and high temperature, but attributed to the pressure-induced Morin transition of hematite or the (weak)ferromagnetic-to-antiferromagnetic phase transition in compressed α-Fe_2O_3 hematite (in Figure S1). Our results are strongly supported by the previously experimental high-pressure magnetic and electrical measurements near 2–5 GPa at room temperature where the pressure dependence of T_M yields as $dT_M/dP = (25 \pm 2)$ K/GPa.[24]

To further explore the pressure-induced anomaly in the shear behavior, the bulk (K_S) and shear (G) moduli as a function of pressure are also plotted in Figure S2. Clearly, the aforementioned pressure-induced anomaly in the shear velocity is also observed in the shear modulus by high-pressure sound velocity measurements. By contrast, this anomalous behavior is absent in the pressure-volume (*P-V*) relation from our static compression experiments combined with synchrotron X-ray diffraction study, further indicating that this anomaly is not a volume-related structural transition at high pressure which is consistent with previously static compression experiments by Liebermann et al.[19]

X-Ray densities and thermoelasticity of α-Fe_2O_3 hematite at high pressure and high temperature

To know more about its high *P-T* behavior, the density changes of hematite with pressures and temperatures derived from the current synchrotron X-ray diffraction data are shown in Figure 3A. Clearly, the density increases with pressures, and

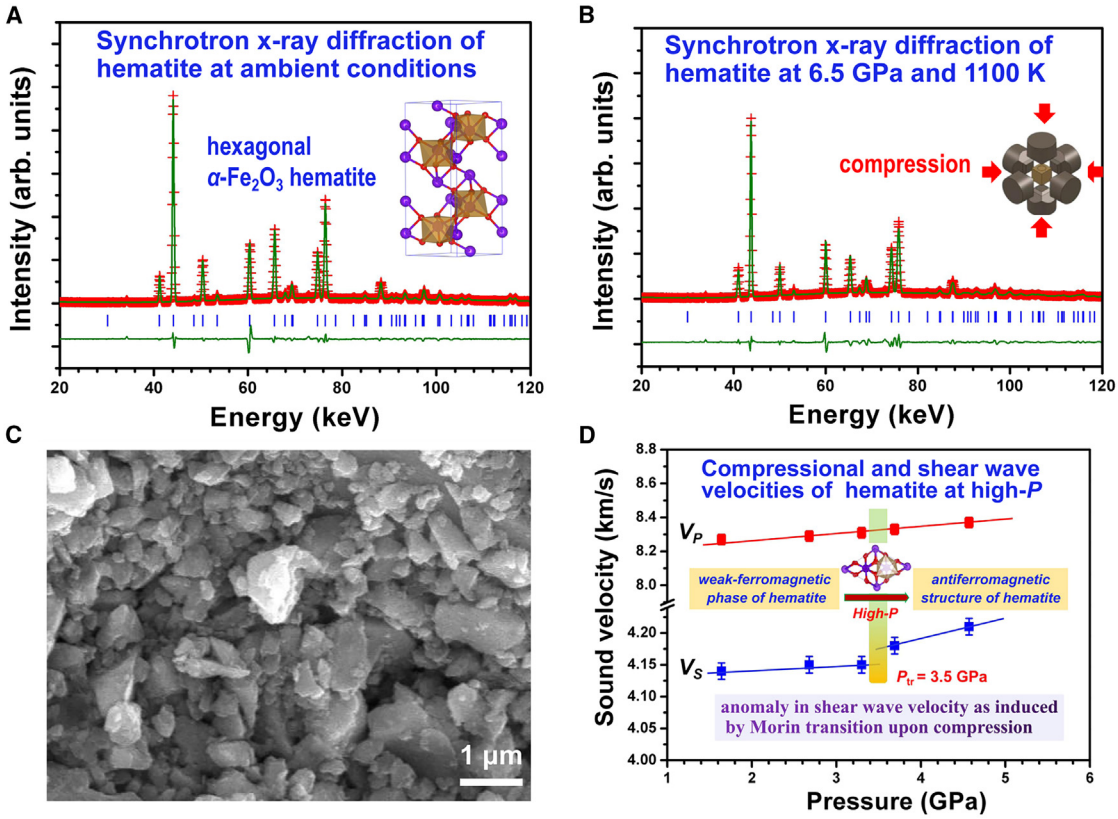

Figure 2. Synchrotron X-ray diffraction, microstructure, and high-pressure acoustic velocities of α-Fe_2O_3 hematite

(A) Synchrotron *in situ* X-ray diffraction pattern of polycrystalline hexagonal α-Fe_2O_3 hematite at ambient conditions used for the current ultrasonic measurements, in comparison with that at the peak *P-T* conditions of 6.5 GPa and 1,100 K (B), showing that the specimen remains in the pure hexagonal hematite structure without the occurrence of any other phases induced by structural phase transition/transformation throughout the current high-pressure and high-temperature experiments. Red crosses and green lines denote the observed and calculated profiles, respectively. The solid green curve at the bottom presents the residuals, and the tick marks correspond to the peak positions of the hexagonal α-Fe_2O_3 hematite; (C) SEM image of the recovered polycrystalline α-Fe_2O_3 hematite for the present sound velocity measurement and synchrotron X-ray study, indicating that the specimen was free of visible microcracks and exhibited an equilibrated and homogeneous microstructure with an average grain size of ~500 nm; (D) Compressional (V_P) and shear (V_S) wave velocities of α-Fe_2O_3 hematite at high pressure after annealing, showing a pronounced pressure-induced anomaly in V_S at ~3.5 GPa, which is attributed to the Morin transition of α-Fe_2O_3 hematite upon compression. The errors are within 0.02 km/s for V_P and 0.01 km/s for V_S. Data with error bars are represented as mean ± SD.

decreases with temperatures without the appearance of dramatic density collapses or jumps throughout the current experiment *P-T* range. When fitting the current densities data to a two-dimensional equation of $\rho = \rho_0 + \frac{\partial \rho}{\partial P}P + \frac{\partial \rho}{\partial T}(T - 300)$, we obtain the ambient-condition density of ρ_0 = 5.251(5) g/cm^3 for hematite, and its pressure and temperature derivatives of $\frac{\partial \rho}{\partial P}$ = 0.027(2) g·cm^{-3}·GPa^{-1} and $\frac{\partial \rho}{\partial T}$ = −0.00016(1) g·cm^{-3}·K^{-1}. Figures 3B and 3C show the compressional and shear wave velocities of Fe_2O_3 hematite along different isotherms at high pressure. It is found that the compressional wave velocity (V_P) exhibits a monotonical increase with pressures up to 6.5 GPa, and a decrease with increasing temperature from 300 K to 1,100 K. Surprisingly, at high temperatures of 500~1,100 K, the shear wave velocity (V_S) shows a gradual temperature-driven softening behavior without the appearance of an apparent Morin-transition-induced discontinuity at room temperature as mentioned in Figure 2D and Figures S1 and S2 where a pressure-induced abnormal shear wave velocity occurs at ~3.5 GPa and room temperature.

Based on the acoustic velocities and densities, the bulk and shear moduli are derived using the equations of $\rho V_P^2 = B_S + 4G/3$ and $\rho V_S^2 = G$ [in Figures 4A and 4B]. Clearly, the room temperature pressure-induced anomaly in V_S at ~3.5 GPa is also observed in the shear moduli at high pressures (in Figure 4B). At temperatures higher than 300 K (e.g., between 500 and 1,100 K), however, this anomalous behavior in the shear moduli is absent, which is consistent the proposed phase boundary of the (weak)ferromagnetic-to-antiferromagnetic phase transition of hematite at high pressures and temperatures (in Figure 1B).

When fitting all the experimental data of the entire *P-T* conditions to the two-dimensional linear equation of $M = M_0 + \frac{\partial M}{\partial P}P + \frac{\partial M}{\partial T}(T - 300)$, we obtained the adiabatic ambient-condition bulk and shear moduli, as well as their pressure and temperature derivatives, yielding K_{S0} = 235.7(8) GPa, G_0 = 87.9(3) GPa, $\partial K_S/\partial p$ = 3.08(23), $\partial G/\partial P$ = 1.45(9), $\partial K_S/\partial T$ = −0.026(2) GPa/K, and $\partial G/\partial T$ = −0.020(1) GPa/K (see Figure 4; Table 1). However, it is worth noting that the aforementioned

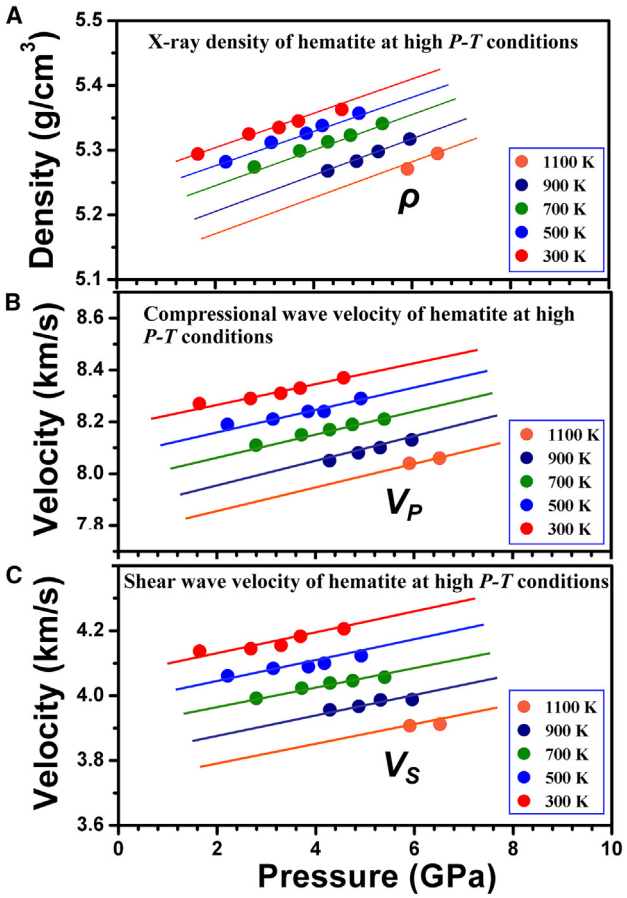

Figure 3. X-ray densities and ultrasonic wave velocities of α-Fe_2O_3 hematite at simultaneously high pressure and high temperature

(A) Density (ρ) of polycrystalline hematite at high pressures and temperatures obtained from the current ultrasonic interferometry measurements and synchrotron X-ray diffraction study, yielding an exploration of zero-pressure density of 5.250(5) g/cm^3 by a two-dimensional linear fitting approach, which is almost the same value as that (ρ = 5.267(1) g/cm^3) of the recovered sample by X-ray diffraction study. The errors in the density from the current experimental study are within ~0.1%; (B) compressional and (C) shear wave velocities of polycrystalline hematite at high pressures and temperatures. The errors are within ~0.3% in the acoustic velocities. Color lines are guides to the eye for isotherms. Data with error bars are represented as mean ± SD.

anomalous behavior in the shear properties of hematite occurs at room temperature (300 K) and pressures above ~3.5 GPa (in Figure 1B; Figures S1 and S2), which is proposed to be attributed to the pressure-induced Morin transition or the (weak)ferromagnetic-to-antiferromagnetic phase transition in compressed Fe_2O_3 hematite. For good understanding, it is thus reasonable to include only the weak-ferromagnetic Fe_2O_3 data during fitting, but exclude the minor phase of antiferromagnetic Fe_2O_3 data (in Figure 1B). Fitting all the weak-ferromagnetic major phase data (antiferromagnetic phase data are excluded during fitting) of hematite to the two-dimensional linear equation, we obtain K_{S0} = 235.4(8) GPa, G_0 = 88.0(3) GPa, $\partial K_S/\partial P$ = 3.29(25), $\partial G/\partial P$ = 1.36(10), $\partial K_S/\partial T$ = −0.027(2) GPa/K, and $\partial G/\partial T$ = −0.019(1) GPa/K (in Figure 4; Table 1). Clearly, the derived bulk and shear moduli, as well as their temperature dependences by using the aforementioned two fits at different *P-T* ranges are almost the same values within their mutual uncertainties (see in Table 1). However, the weak-ferromagnetic α-Fe_2O_3 exhibits a slightly stronger pressure dependence of bulk modulus $\partial K_S/\partial P$ = 3.29, but a weaker value of $\partial G/\partial P$ = 1.36, which are compared to those of $\partial K_S/\partial P$ = 3.08 and $\partial G/\partial P$ = 1.45 for the nominal two phases (major weak-ferromagnetic + minor antiferromagnetic phases) of Fe_2O_3 at the entire *P-T* range.

DISCUSSION

Our experimentally obtained elasticity of bulk and shear moduli of α-Fe_2O_3 hematite, as well as their pressure and temperature dependences are summarized in Table 1 for comparison with those from the previous studies.[9,19–21,29–31] It is found that our obtained adiabatic bulk modulus of K_{S0} = 235.4(8) GPa for weak-ferromagnetic α-Fe_2O_3 hematite (in Figure 1B) is in good agreement with the in-house acoustic measurement value of K_{S0} = 241.7 GPa reported by Liebermann et al.,[19] and also consistent with the synchrotron-based static compression experiments of isothermal bulk modulus of K_0 = 230–231 GPa within mutual uncertainties.[9,21,31] By contrast, however, the above-mentioned adiabatic bulk modulus of K_{S0} = 235.4(8) GPa is about 9~12% higher than the theoretical value of ~215 GPa,[29] and the previously acoustic result of K_{S0} = 206.6 GPa for the antiferromagnetic α-Fe_2O_3 hematite.[20] This difference may be due to the use of different experimental techniques for measurements and the well-known debinding of generalized gradient approximation (GGA) for theoretical calculations. For shear modulus, our experimentally obtained G_0 = 88.0 GPa is consistent well with the previous acoustic study (G_0 = 91.0 GPa) for antiferromagnetic phase by Liebermann et al.[20]

As shown in Table 1, the pressure dependence of bulk modulus $\partial K_S/\partial P$ = 3.29(25) for weak ferromagnetic α-Fe_2O_3 hematite from the current synchrotron-based acoustic measurements is in good agreement with the value of $\partial K_S/\partial P$ = ~3.5 by Olsen et al.[9] and Catti et al.[31] from the previous static compression experiments, as well as the theoretically predicted $\partial K_S/\partial P$ = 3.1.[29] However, the pressure dependence of bulk modulus ($\partial K_S/\partial P$ = 3.1) is significantly lower than the acoustic value of $\partial K_S/\partial P$ = 4.53 for antiferromagnetic phase of α-Fe_2O_3 by Liebermann et al.[20] This large discrepancy may be due to the narrow pressure range (the maximum pressure is only limited to 3 kbar) and/or the precision of calibrated pressures used in the previous in-house/offline acoustic measurements.[20] By contrast, the experimental value of $\partial G/\partial P$ = 1.36(10) in weak-ferromagnetic hematite is significantly higher than that ($\partial G/\partial P$ = 0.73) for the antiferromagnetic α-Fe_2O_3.[22]

As major candidates of the Earth's mantle and core, it is of great importance to understand the sound velocities, elastic moduli and their pressure derivatives for typical Fe-O minerals with various Fe/O ratios (e.g., Fe_2O_3 hematite, Fe_3O_4 magnetite and FeO wüstite). As shown in Figure 5A, both elastic compressional (V_P) and shear (V_S) wave velocities decrease with the increasing Fe/O ratios in Fe-O minerals. It is found that the values of V_P and V_S in α-Fe_2O_3 hematite are about ~25% and ~30% higher than those for $Fe_{0.95}O$ wüstite,[39] respectively. This

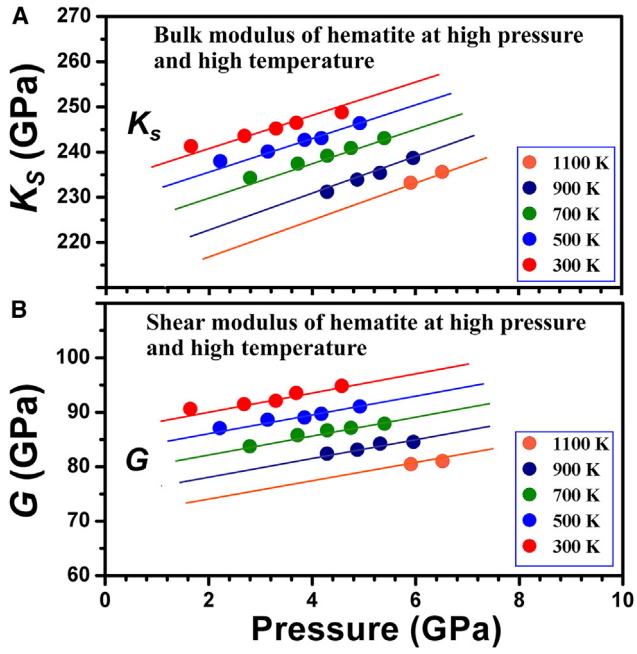

Figure 4. Elasticity of α-Fe_2O_3 hematite at simultaneously high pressure and high temperature

(A) Bulk and (B) shear moduli of polycrystalline hematite at high pressures and temperatures. The errors are within ~1.5% in the elastic moduli. Color lines are guides to the eye for isotherms. Data with error bars are represented as mean ± SD.

composition-dependent trends in the acoustic velocities are also observed in the elasticity of K_S and G, as shown in Figure 5B.

To further explore the high-pressure elasticity of iron-bearing oxides, the pressure dependences of bulk and shear moduli for hematite are shown in Figure 5C, as compared with those for magnetite and wüstite by Jacobsen et al.[39] Clearly, the Fe_3O_4 magnetite possesses a weaker value of $\partial K_S/\partial P \approx 3.0$ as compared with those for hematite ($\partial K_S/\partial P \approx 3.3$) and wüstite ($\partial K_S/\partial P$ = 3.7). By contrast, the pressure derivative of shear moduli ($\partial G/\partial P$) decreases with increasing Fe/O ratios, and it exhibits a negative value of −0.22 and −0.23 for magnetite and wüstite,[39] respectively. This shear softening behavior is likely due to the strong magnetoelastic coupling in magnetite and wüstite, which indicates their structural instability at high pressure.

It is well accepted that the bulk modulus value is inversely proportional to the unit-cell volume, and the product of $K_0 \times V_0$ should be approximately constant for similar-structured materials.[45] As shown in Figure 5D, the ambient-condition bulk modulus (K_0) is plotted as a function of the reciprocal volume of the formula unit [1/(V_0/Z)] (where Z is the number of formula units in the cell) for typical corundum-structured oxides (Z = 6), yielding an apparent linear relation in Figure 5D. We find that the experimental K_0-[1/(V_0/Z)] relations for α-Fe_2O_3 hematite apparently agree well with the linear behavior in other corundum-structured materials such as Al_2O_3,[40] Cr_2O_3,[41] Ti_2O_3,[42] Ga_2O_3[43] and V_2O_3[44] (seen in Figure 5D).

With high abundance of iron and oxygen in the Earth's crust and mantle, iron oxides are considered to be key minerals which make significant contributions to the properties of the Earth. Understanding sound velocities and elasticity of iron oxides at extreme high P-T conditions plays an important role in interpreting the structural stability, composition, and mineralogy of the Earth's interiors. Our results demonstrate that the structural stability and sound velocities/elasticity for typical Fe-O minerals (e.g., Fe_3O_4 magnetite,[32] Fe_2O_3 hematite[19,20] and FeO wüstite[39]) are quite different which is very sensitive to the Fe/O ratio at various pressures and temperatures, probably providing significant consequences for modeling of the Earth's interior. It is known that the temperature of the Earth's crust interiors is far above the Morin transition of T_M ~250 K at ambient pressure but doesn't exceed the Curie temperature of ~948 K for hematite.[16–18] We thus reasonably assume that hematite present in Earth's crust is in the (weak)ferromagnetic state. For the Earth, only the first kilometers of crust may be affected by the process with the pressure wave of ~2 GPa. This effect eventually resulted in a pressure-induced anomaly or demagnetization at pressures above 1.5 GPa and room temperature, which is probably the reason for our observed anomaly in the shear properties at ~3.5 GPa and 300 K in hematite mineral, or for the pressure demagnetization in hematite-bearing rocks.[24] The different transition-pressures may be attributed to the use of different experimental techniques, or the effects of nonhydrostatic stress accumulated in the high-pressure chamber which may significantly affect the pressure sensitivity of the Morin transition as proposed by Coe et al.[46]

Table 1. Summary of the elasticity of α-Fe_2O_3 hematite, compared with the previously experimental and theoretical results

Minerals	K_{S0} (GPa)	G_0 (GPa)	$\partial K_S/\partial P$	$\partial G/\partial P$	$\partial K_S/\partial T$ (GPa/K)	$\partial G/\partial T$ (GPa/K)	Reference
Fe_2O_3 hematite	235.4(8)	88.0(3)	3.29(25)	1.36(10)	−0.027(2)	−0.019(1)	*This study* (weak-ferromagnetic phase)
	235.7(8)	87.9(3)	3.08(23)	1.45(9)	−0.026(2)	−0.020(1)	*This study* (entire P-T range fitting)
	215	–	3.1	–	–	–	Wilson et al.,Theor.[29]
	241.7	–	4.5[a]	–	–	–	Liebermann et al.[19] (weak-ferromagnetic α-Fe_2O_3)
	206.6	91.0	4.53(13)	0.73(3)	–	–	*Liebermann*et al.[20] (antiferromagnetic phase)
	231(10)	–	4.0[a]	–	–	–	Sato and Akimoto[21] (weak-ferromagnetic α-Fe_2O_3)
	230(5)	–	3.5(6)	–	–	–	Olsen et al.[9]
	230	–	3.5	–	–	–	Catti et al.[31]

[a]fixed values.

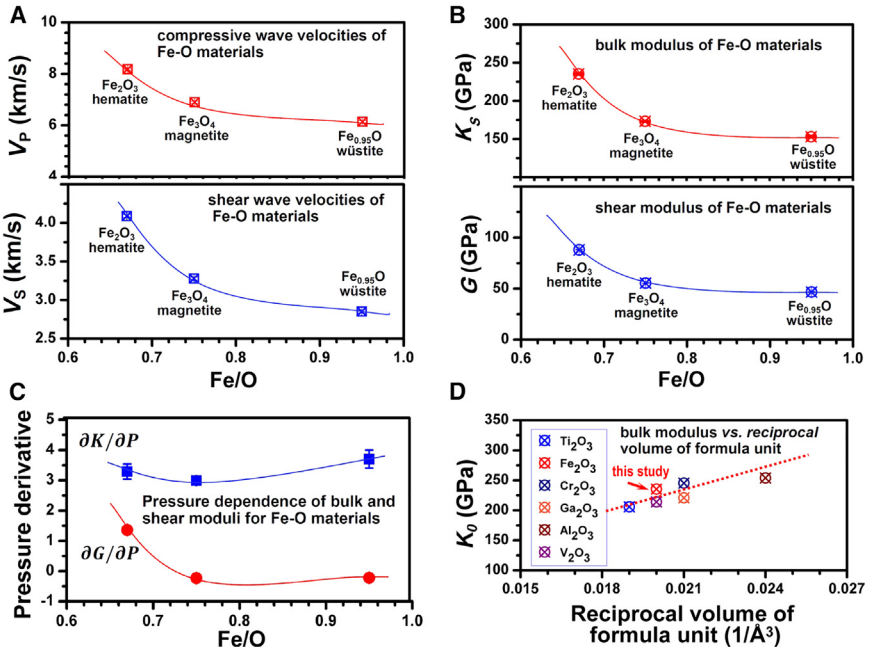

Figure 5. Acoustic velocities, elasticity and their pressure dependences of Fe-O compounds, as well as the ambient-condition bulk moduli of corundum-structured oxides

(A) Compressional (V_P) and shear (V_S) wave velocities of iron oxides with various Fe-O ratios; (B) Bulk (K_S) and shear (G) moduli of iron oxides with various Fe/O ratios; (C) Pressure derivatives for bulk (K_S) and shear (G) moduli of iron oxides; The errors are within~0.3% and ~1.5% in the acoustic velocities and elastic moduli, respectively; (D) Relations between the bulk modulus (K) and reciprocal volume of the formula unit [$1/(V_0/Z)$] for corundum-structured oxides. We used the most accurate data, *e.g.*, K_0 = 235.4 GPa and V_0/Z = 50.35 Å^3 for Fe_2O_3 hematite from this study; K_0 = 254 GPa and V_0/Z = 42.47 Å^3 for Al_2O_3 from[40]; K_0 = 245.4 GPa and V_0/Z = 48.12 Å^3 for sing-crystal Cr_2O_3[41]; K_0 = 206 GPa and V_0/Z = 52.28 Å^3 for powdered Ti_2O_3[42];K_0 = 206 GPa and V_0/Z = 52.28 Å^3 for powdered Ga_2O_3[43];K_0 = 206 GPa and $V_0/Z \approx$ 50.35 Å^3 for powdered V_2O_3.[44] Data with error bars are represented as mean ± SD.

This magnetoelastic interaction is not unique to hematite among minerals of geophysical interest, but includes all magnetically ordered materials such as FeO, CoO, MnO, NiO and Cr_2O_3,[44] which opens the question of interactions when sound velocities and elasticity are measured using synchrotron-based ultrasonic interferometry technique. Generally, the order-disorder transition temperatures for the magnetic oxides are formulated as a function of pressure. When studying minerals' and/or rock's magnetism, it is often necessary to understand the detailed spin orientation. Using synchrotron-based ultrasonic interferometry and magnetic property measurements at high pressures and/or temperatures, it is possible to diagnose the orientations of the spins and the nature of the domain structure, sound velocities and elasticity, yielding important information on the spin alignment by studying spin wave-phonon interactions. The special importance to geophysics may be due to elasticity discontinuities of crystals across magnetic phase transitions. To date, considerable attention has been devoted to studying elastic behavior in the region of order-disorder transition temperatures, but much work remains to be done. Especially, the pressure effects of order-order transitions such as the Morin transition and high *P-T* velocities/elasticity in Fe_2O_3 hematite cannot be overlooked.

Acoustic velocities, elasticity, and phase transition of Fe_2O_3 hematite, for the first time, are studied at simultaneously high pressure and high temperature using ultrasonic interferometry in conjunction with synchrotron X-ray diffraction and X-radiographic imaging techniques. Here, we find an unexpected pressure-induced anomaly in the shear behavior of compressed hematite at ~3.5 GPa and room temperature, which is attributed to the (weak)ferromagnetic-to-antiferromagnetic Morin transition at high pressure. For compressional wave velocities, however, this anomalous discontinuity is absence with increasing pressure and temperature up to 6.5 GPa and 1,100 K. On the other hand, the bulk and shear moduli, as well as their pressure and temperature derivatives for weak-ferromagnetic Fe_2O_3 hematite yield K_{S0} = 235.5(8) GPa, G_0 = 88.0(3) GPa, $\partial K_S/\partial P$ = 3.29(25), dG/dP = 1.36(10), $\partial K_S/\partial T$ = −0.027(2) GPa/K, and $\partial G/\partial T$ = −0.019(1) GPa/K. Moreover, some elasticity-related properties, such as Debye temperature, Poisson's ratio, and Young's modulus of hematite at high pressure and high temperature are also reported. The underlying mechanism of pressure-induced anomaly at high temperature and new high-*P* thermoelasticity of Fe_2O_3 hematite are of significant importance for its geophysical and materials science implications in the high-pressure behavior of corundum-structured oxides and for gaining a good understanding of the mechanism for phase-transition-induced shear anomalies in Fe-O materials at high pressure and high temperature.

Limitations of the study

Synchrotron-based ultrasonic wave velocity measurements on polycrystalline α-Fe_2O_3 hematite are performed at simultaneously high pressures and temperatures up to 6.5 GPa and 1,100 K. In this study, we report the pressure-induced anomalies in the shear properties of α-Fe_2O_3 and explore the underlying mechanism. The limitation is that the experimental peak pressure and temperature of this study is still not as high as those of the Earth's mantle conditions.

RESOURCE AVAILABILITY

Lead contact

Requests for further information should be directed to the lead contact, Yongtao Zou (zouyongtao@sztu.edu.cn).

Materials availability

This study did not generate new materials or new unique reagents.

Data and code availability

- All data can be obtained from the lead contact, provided the request is reasonable.
- This paper does not report original code.
- Any additional information required to reanalyze the data reported in this paper is available from the lead contact upon request.

ACKNOWLEDGMENTS

This work was supported by the Joint Funds of the National Natural Science Foundation of China and China Academy of Engineering Physics (NSAF) (no. U2030110), National Natural Science Foundation of China (no. 11872198), Shenzhen Science and Technology Program (grant nos. JCYJ202103 24121405014, JCYJ20190813103201662, ZDSYS20200811143600001), Runyuan Young Principle Investigator (PI) of Shenzhen Technology University (SZTU) (grant no. RY2022010), the Key Research Platforms and Research Projects of Universities in Guangdong Province (grant no. 2020ZDZX2035), Natural Science Foundation of Top Talent of Shenzhen Technology University (SZTU) (grant no. 2019202), Guangdong Province Key Construction Discipline Scientific Research Capacity Improvement Project (grant no. 2021ZDJS107), and also partially supported by the Open Foundation of United Laboratory of High-Pressure Physics and Earthquake Science, Institute of Education Sciences, China Earthquake Administration.

AUTHOR CONTRIBUTIONS

Y.Z. proposed and designed the research; Y.Z., Y.L., and H.C. carried out the high *P-T* experiments and data analysis; Y.Z., C.Z., P.W., H.C., Y.L., C.Z., and T.I. wrote, reviewed, and edited the paper.

DECLARATION OF INTERESTS

The authors declare no competing interests.

STAR★METHODS

Detailed methods are provided in the online version of this paper and include the following:

- KEY RESOURCES TABLE
- EXPERIMENTAL MODEL AND STUDY PARTICIPANT DETAILS
- METHOD DETAILS
  - Synthesis and characterization
  - Synchrotron-based ultrasonic measurements at high P-T conditions in a large volume press
  - Calculations of sound velocities, bulk and shear moduli, as well as their pressure and temperature dependences
- QUANTIFICATION AND STATISTICAL ANALYSIS

SUPPLEMENTAL INFORMATION

Supplemental information can be found online at https://doi.org/10.1016/j.isci.2025.111905.

Received: July 4, 2024
Revised: December 7, 2024
Accepted: January 23, 2025
Published: January 28, 2025

REFERENCES

1. Bykova, E., Dubrovinsky, L., Dubrovinskaia, N., Bykov, M., McCammon, C., Ovsyannikov, S.V., Liermann, H.-P., Kupenko, I., Chumakov, A.I., Rüffer, R., et al. (2016). Structural complexity of simple Fe_2O_3 at high pressures and temperatures. Nat. Commun. *7*, 10661.
2. Tuček, J., Machala, L., Ono, S., Namai, A., Yoshikiyo, M., Imoto, K., Tokoro, H., Ohkoshi, S.i., and Zbořil, R. (2015). Zeta-Fe_2O_3-A new stable polymorph in iron (III) oxide family. Sci. Rep. *5*, 15091.
3. Shim, S.H., Bengtson, A., Morgan, D., Sturhahn, W., Catalli, K., Zhao, J., Lerche, M., and Prakapenka, V. (2009). Electronic and magnetic structures of the postperovskitetype Fe_2O_3 and implications for planetary magnetic records and deep interiors. Proc. Natl. Acad. Sci. *106*, 5508–5512.
4. Dobson, D.P., and Brodholt, J.P. (2005). Subducted banded iron formations as a source of ultralow-velocity zones at the core-mantle boundary. Nature *434*, 371–374.
5. Ovsyannikov, S.V., Morozova, N.V., Karkin, A.E., and Shchennikov, V.V. (2012). High-pressure cycling of hematite α-Fe_2O_3: nanostructuring, in situ electronic transport, and possible charge disproportionation. Phys. Rev. B *86*, 205131.
6. Badro, J., Fiquet, G., Struzhkin, V.V., Somayazulu, M., Mao, H.k., Shen, G., and Le Bihan, T. (2002). Nature of the high-pressure transition in Fe_2O_3 hematite. Phys. Rev. Lett. *89*, 205504.
7. Pasternak, M.P., Rozenberg, G.K., Machavariani, G.Y., Naaman, O., Taylor, R.D., and Jeanloz, R. (1999). Breakdown of the Mott-Hubbard state in Fe_2O_3: A first-order insulator-metal transition with collapse of magnetism at 50 GPa. Phys. Rev. Lett. *82*, 4663–4666.
8. Rozenberg, G.K., Dubrovinsky, L.S., Pasternak, M.P., Naaman, O., Le Bihan, T., and Ahuja, R. (2002). High-pressure structural studies of hematite Fe_2O_3. Phys. Rev. B *65*, 064112.
9. Olsen, J.S., Cousins, C.S.G., Gerward, L., Jhans, H., and Sheldon, B.J. (1991). A study of the crystal structure of Fe_2O_3 in the pressure range up to 65 GPa using synchrotron radiation. Phys. Scr. *43*, 327–330.
10. Ito, E., Fukui, H., Katsura, T., Yamazaki, D., Yoshino, T., Aizawa, Y., Kubo, A., Yokoshi, S., Kawabe, K., Zhai, S., et al. (2009). Determination of high-pressure phase equilibria of Fe_2O_3 using the Kawai-type apparatus equipped with sintered diamond anvils. Am. Mineral. *94*, 205–209.
11. Bykova, E., Bykov, M., Prakapenka, V., Konôpková, Z., Liermann, H.-P., Dubrovinskaia, N., and Dubrovinsky, L. (2013). Novel high pressure monoclinic Fe_2O_3 polymorph revealed by single-crystal synchrotron X-ray diffraction studies. High Press. Res. *33*, 534–545.
12. Ono, S., and Funakoshi, K. (2005). In situ X-ray observation of phase transformation in Fe_2O_3 at high pressures and high temperatures. J. Phys. Condens. Matter *66*, 269–276.
13. Liu, H., Caldwell, W.A., Benedetti, L.R., Panero, W., and Jeanloz, R. (2003). Static compression of α-Fe_2O_3: linear incompressibility of lattice parameters and high-pressure transformations. Phys. Chem. Miner. *30*, 582–588.
14. Schouwink, P., Dubrovinsky, L., Glazyrin, K., Merlini, M., Hanfland, M., Pippinger, T., and Miletich, R. (2011). High-pressure structural behavior of α-Fe_2O_3 studied by single-crystal X-ray diffraction and synchrotron radiation up to 25 GPa. Am. Mineral. *96*, 1781–1786.
15. Pauling, L., and Hendricks, S.B. (1925). The crystal structures of hematite and corundum. J. Am. Chem. Soc. *47*, 781–790.
16. Morrish, A.H. (1994). Canted Antiferromagnetism: Hematite (World Scientific).
17. Shull, C.G., Strauser, W.A., and Wollan, E.O. (1951). Neutron diffraction by paramagnetic and antiferromagnetic substances. Physiol. Rev. *83*, 333–345.
18. Amin, N., and Arajs, S. (1987). Morin temperature of annealed submicronic α-Fe_2O_3 particles. Phys. Rev. B *35*, 4810–4811.
19. Liebermann, R.C., and Maasch, K.A. (1986). Acoustic and static compression experiments on the elastic behavior of hematite. J. Geophys. Res. *91*, 4651–4656.
20. Liebermann, R.C., and Schreiber, E. (1968). Elastic constants of polycrystalline hematite as a function of pressure to 3 kilobars. J. Geophys. Res. *73*, 6585–6590.

21. Sato, Y., and Akimoto, S.i. (1979). Hydrostatic compression of four corundum-type compounds: α-Al_2O_3, V_2O_3, Cr_2O_3, and α-Fe_2O_3. J. Appl. Phys. *50*, 5285–5291.

22. Parise, J.B., Locke, D.R., Tulk, C.A., Swainson, I., and Cranswick, L. (2006). The effect of pressure on the Morin transition in hematite (α-Fe_2O_3). Physica B *385–386*, 391–393.

23. Syono, Y., Ito, A., Morimoto, S., Suzuki, T., Yagi, T., and Akimoto, S.i. (1984). Mössbauer study on the high pressure phase of Fe_2O_3. Solid State Commun. *50*, 97–100.

24. Bezaeva, N.S., Demory, F., Rochette, P., Sadykov, R.A., Gattacceca, J., Gabriel, T., and Quesnel, Y. (2015). The effect of hydrostatic pressure up to 1.61 GPa on the Morin transition of hematite-bearing rocks: Implications for planetary crustal magnetization. Geophys. Res. Lett. *42*, 066306.

25. Greenberg, E., Leonov, I., Layek, S., Konopkova, Z., Pasternak, M.P., Dubrovinsky, L., Jeanloz, R., Abrikosov, I.A., and Rozenberg, G.K. (2018). Pressure-induced site-selective Mott insulator-metal transition in Fe_2O_3. Phys. Rev. X *8*, 031059.

26. Sanson, A., Kantor, I., Cerantola, V., Irifune, T., Carnera, A., and Pascarelli, S. (2016). Local structure and spin transition in Fe_2O_3 hematite at high pressure. Phys. Rev. B *94*, 014112.

27. Srivastava, S., Pandey, A.K., and Dixit, C.K. (2023). Theoretical prediction of Grüneisen parameter for γ-Fe_2O_3. Comput. Condens. Matter. *35*, e00801.

28. Srivastava, S., Singh, P., Pandey, A.K., Dixit, C.K., Pandey, K., and Tripathi, S. (2023). Equation of states at extreme compression ranges: pressure and bulk modulus as an example. Mater. Open *01*, 2350007.

29. Wilson, N.C., and Russo, S.P. (2009). Hybrid density functional theory study of the high-pressure polymorphs of α-Fe_2O_3 hematite. Phys. Rev. B *79*, 094113.

30. Finger, L.W., and Hazen, R.M. (1980). Crystal structures and isothermal compression of Fe_2O_3, Cr_2O_3 and V_2O_3 to 50 kbars. J. Appl. Phys. *51*, 5362–5367.

31. Catti, M., Valerio, G., and Dovesi, R. (1995). Theoretical study of electronic, magnetic, and structural properties of α-Fe_2O_3 (hematite). Phys. Rev. B *51*, 7441–7450.

32. Zou, Y., Zhang, W., Chen, T., Li, X.a., Wang, C.-H., Qi, X., Wang, S., Yu, T., Liu, B., Wang, Y., et al. (2018). Thermally induced anomaly in the shear behavior of Fe_3O_4 magnetite at high pressure. Phys. Rev., A. *10*, 024009.

33. Zou, Y., Li, Y., Chen, H., Welch, D., Zhao, Y., and Li, B. (2018). Thermoelasticity and anomalies in the pressure dependence of phonon velocities in niobium. Appl. Phys. Lett. *112*, 011901.

34. Liu, W., Li, B., Wang, L., Zhang, J., and Zhao, Y. (2007). Elasticity of ω-phase zirconium. Phys. Rev. B *76*, 144107.

35. Zou, Y., Irifune, T., Gréaux, S., Whitaker, M., Shinmei, T., Ohfuji, H., Negishi, R., and Higo, Y. (2012). Elasticity and sound velocities of polycrystalline $Mg_3Al_2(SiO_4)_3$ garnet up to 20 GPa and 1700 K. J. Appl. Phys. *112*, 14910.

36. Zou, Y., Gréaux, S., Irifune, T., Li, B., and Higo, Y. (2013). Unusual pressure effect on the shear modulus in $MgAl_2O_4$ spinel. J. Phys. Chem. C *117*, 24518–24526.

37. Irifune, T., Higo, Y., Inoue, T., Kono, Y., Ohfuji, H., and Funakoshi, K. (2008). Sound velocities of majorite garnet and the composition of the mantle transition region. Nature *451*, 814–817.

38. Teja, A.S., and Koh, P.-Y. (2009). Synthesis, properties, and applications of magnetic iron oxide nanoparticles. Prog. Cryst. Growth Charact. Mater. *55*, 22–45.

39. Jacobsen, S.D., Spetzler, H., Reichmann, H.J., and Smyth, J.R. (2004). Shear waves in the diamond-anvil cell reveal pressure-induced instability in (Mg,Fe)O. Proc. Natl. Acad. Sci. *101*, 5867–5871.

40. Syassen, K. (2008). Ruby under pressure. High Press. Res. *28*, 75–126.

41. Kantor, A., Kantor, I., Merlini, M., Glazyrin, K., Prescher, C., Hanfland, M., and Dubrovinsky, L. (2012). High-pressure structural studies of eskolaite by means of single-crystal X-ray diffraction. Am. Mineral. *97*, 1764–1770.

42. Nishio-Hamane, D., Katagiri, M., Niwa, K., Sano-Furukawa, A., Okada, T., and Yagi, T. (2009). A new high-pressure polymorph of Ti_2O_3: implication for high-pressure phase transition in sesquioxides. High Press. Res. *29*, 379–388.

43. Lipinska-Kalita, K.E., Kalita, P.E., Hemmers, O.A., and Hartmann, T. (2008). Equation of state of gallium oxide to 70 GPa: Comparison of quasihydrostatic and nonhydrostatic compression. Phys. Rev. B *77*, 094123.

44. McWhan, D.B., and Remeika, J.P. (1970). Metal-insulator transition in $(V_{1-x}Cr_x)_2O_3$. Phys. Rev. B *2*, 3734–3750.

45. Anderson, D.L., and Anderson, O.L. (1970). The bulk modulus-volume relationship for oxides. J. Geophys. Res. *75*, 3494–3500.

46. Coe, R.S., Egli, R., Gilder, S.A., and Wright, J.P. (2012). The thermodynamic effect of nonhydrostatic stress on the Verwey transition. Earth. Planet. Sci. Lett. *319–320*, 207–217.

STAR★METHODS

KEY RESOURCES TABLE

REAGENT or RESOURCE	SOURCE	IDENTIFIER
Chemicals, peptides, and recombinant proteins		
α-Fe_2O_3 hematite	Lieberman et al.[19,20]	N/A
Deposited data		
Structure of compound	This paper; (Inorganic Crystal Structure Database)	ICSD: 82137
Software and algorithms		
GSAS software package	NIST Center for Neutron Research	https://www.ncnr.nist.gov/instruments/bt1/bt1_downloads.html
OriginLab	Analyze and graph	https://www.originlab.com
VESTA software package	JP-Minerals	https://jp-minerals.org/vesta/en/

EXPERIMENTAL MODEL AND STUDY PARTICIPANT DETAILS

In this study, we do not use experimental models typical in the life sciences.

METHOD DETAILS

Synthesis and characterization

The polycrystalline α-Fe_2O_3 hematite specimen used in the current study was provided by Robert C. Liebermann (State University of New York at Stony Brook, USA), which was fabricated using a vacuum hot press. Prior to the current synchrotron-based elastic wave velocity measurements at high pressure and high temperature, the crystal structure of as-measured polycrystalline hematite specimen was characterized by X-ray diffractometer (Rigaku, Japan). The bulk density of the well-sintered α-Fe_2O_3 hematite is measured using the Archimedes' immersion method. The morphology and the chemical composition of α-Fe_2O_3 hematite specimen were further characterized using a scanning electron microscopy combined with an energy dispersive spectrometer (SEM- EDS: Nova NanoSem450).

Synchrotron-based ultrasonic measurements at high P-T conditions in a large volume press

Elastic compressional (*P*) and shear (*S*) wave velocities of polycrystalline α-Fe_2O_3 hematite were measured at simultaneously high pressure and high temperature using ultrasonic interferometry in conjunction with synchrotron X-ray diffraction and x-radiographic imaging techniques in a large volume press at the National Synchrotron Light Source (NSLS), Brookhaven National Laboratory, USA. The experimental setup and the pressure-temperature (*P-T*) path for the present synchrotron-based experiments are shown in Figures 1A and 1B, where each point represents a pressure-temperature (*P-T*) condition that X-ray diffraction and acoustic data for α-Fe_2O_3 hematite are collected. Details of the high *P-T* cell assembly can be found elsewhere.[32–37] Briefly, a mixture of amorphous boron and epoxy resin was used as the pressure-transmitting medium, and a graphite furnace was used as a heating element. The temperature was directly measured by a W/Re25%-W/Re3% thermocouple, which was located next to the α-Fe_2O_3 hematite specimen. The specimen was embedded in a mixture of NaCl+ *h*-BN powder (10:1 wt %), providing hydrostatic environments for the sample.

A dual-mode $LiNbO_3$ transducer (10° Y-cut) was mounted outside the pressure chamber, which can generate and receive *P* and *S* waves simultaneously. Travel times were measured using the transfer function method with a standard deviation of ~0.4 ns for the *S* wave and ~0.2 ns for the *P* wave.[32–37] The sample length at high pressure and/or high temperature was directly derived by the x-radiographic imaging method. During our experiments, X-ray diffraction patterns for both the specimen and NaCl pressure marker were collected using a solid-state detector with a diffraction angle of $2\theta \approx 6.45^{\circ}$. The X-ray diffraction patterns of the sample were refined to determine the unit-cell volumes and densities.

Calculations of sound velocities, bulk and shear moduli, as well as their pressure and temperature dependences

On the basis of the travel times (t_p and t_s for both compressional and shear waves) and sample length (*L*) at various pressures and temperature, the corresponding sound velocities of compressional (V_P) and (V_S) waves for polycrystalline α-Fe_2O_3 hematite are calculated using the equations of $V_P = L/t_p$ and $V_S = L/t_s$, respectively. The elasticity of bulk ($\rho V_P^2 = K_S + 4G/3$) and shear ($\rho V_S^2 = G$) moduli are calculated from *P* and *S* wave velocities and X-ray densities. All the data in the entire *P-T* range are fitted simultaneously to obtain the adiabatic bulk and shear modulus at ambient conditions, as well as their pressure and temperature dependences using

the two-dimensional linear equation of $M = M_0 + \frac{\partial M}{\partial P}P + \frac{\partial M}{\partial T}(T - 300)$, where P is pressure (in GPa) and T is the temperature (in K).

QUANTIFICATION AND STATISTICAL ANALYSIS

Synchrotron X-ray diffraction data are processing by using the GSAS software. Data analysis was performed using Excel (Microsoft) and Origin (OriginLab). Error bars in Figures 2C, 3, 4, and 5 are obtained by the propagation of errors of measured pressure (P), temperature (T), travel times(t_p *and* t_s), sample length (L), and unit-cell volumes (V) at various pressures and temperatures. Errors of the parameters in Table 1 are derived by fitting the entire high P-T data to the two-dimensional linear equation of $M = M_0 + \frac{\partial M}{\partial P}P + \frac{\partial M}{\partial T}(T - 300)$. The errors in the measured pressure (P), temperature (T), travel times (t_p *and* t_s), unit-cell volumes (V), and sample length (L) are derived by the fitting errors from synchrotron X-ray diffraction patterns and X-radiography images of polycrystalline α-Fe_2O_3 hematite specimen at various pressures and temperatures.